Pure Appl. Chem., Vol. 84, No. 3, pp. 495–508, 2012.
http://dx.doi.org/10.1351/PAC-CON-11-07-12

Laser electrodispersion as a new chlorine-free method for the production of highly effective metal-containing supported catalysts*

Ekaterina S. Lokteva[1,‡], Anton A. Peristyy[1], Natalia E. Kavalerskaya[1], Elena V. Golubina[1], Lada V. Yashina[1], Tatiana N. Rostovshchikova[1], Sergey A. Gurevich[2], Vladimir M. Kozhevin[2], Denis A. Yavsin[2], and Valery V. Lunin[1]

[1]Department of Chemistry, Lomonosov Moscow State University, Moscow, Russia; [2]Ioffe Physical-Technical Institute, Russian Academy of Sciences, St. Petersburg, Russia

Abstract: Laser electrodispersion (LED) of metals is a promising technique for the preparation of heterogeneous catalysts as an alternative to wet impregnation of supports with the corresponding salt solutions. The LED technique can be used to deposit highly active chloride- and nitrate-free metal nanoparticles onto carbon or oxide supports. We report preparation and properties of new Ni-, Pd-, and Au-containing alumina-supported catalysts with low metal loadings (10^{-3}–10^{-4} % mass) and their comparison with the previously studied carbon (Sibunit) supported systems. The catalysts demonstrate high stability and extremely high specific catalytic activity (by 2–3 orders of magnitude higher than for traditional catalysts) in the gas-phase hydrodechlorination (HDC) of chlorobenzene (CB).

Keywords: alumina-supported Au; alumina-supported Ni; bimetallic Au–Ni catalyst; carbon-supported Ni; carbon-supported Pd; chlorine-free catalyst; chlorobenzene; hydrodechlorination; laser electrodispersion.

INTRODUCTION

The routine and well-developed way to produce supported catalysts is based on the support impregnation with the corresponding metal salts (mainly chlorides or nitrates). After drying, calcination, and reduction, catalytically active metal nanoparticles are obtained on the surface and/or in the bulk of the support material. This method is quite simple and widely applied [1,2]. Its recent developments allow precise control of the mean particle size and the size distribution, and in certain cases even the particle shape, the oxidation degree, and the interaction with the support material (e.g., anchoring). However, there are a number of disadvantages that motivate the search for alternative catalyst production protocols. Such disadvantages may be summarized as follows:

1. The use of metal salts, predominantly chlorides and nitrates, as source materials. First, this generates a need for the use of Cl chemistry to produce the chlorides of catalytically active metals (noble metals and other Group VIII metals, Cu, Ag, etc.); second, the problem of toxic Cl deriv-

Pure Appl. Chem.* **84, 411–860 (2012). A collection of invited papers for the IUPAC project 2008-016-1-300 "Chlorine-free Synthesis for Green Chemistry".
‡Corresponding author

atives venting to the atmosphere during calcination arises. Similar problems have to be resolved for nitrates owing to the formation of nitrogen oxides.

2. A multistage production process, which includes impregnation, drying, calcinations, and reduction, with all stages being energy-consuming.
3. Typically, a very broad metal particle size distribution in the catalyst. It has been established that often only particles of a certain size are catalytically active, and most frequently they are of nanometer scale size. In addition, production of very small particles makes the noble metal catalysts essentially cheaper because of the surface-to-volume ratio of the active metal atoms. Thus, for small particles the noble metals are spent in the most efficient manner.
4. The fact that the metal particles are distributed not only on the outer surface of the support material but also in the bulk. For many industrial processes, the metal particles in the bulk of the support are not accessible for the reactant adsorption, and the resulting number of the active centers is much lower compared to systems where the metal is fully distributed on the outer surface of the support particles or pellets.

Many other "wet chemistry" approaches also employ metal salts. Recent development of new procedures for metal precursor deposition (e.g., deposition-precipitation, reverse micelle impregnation, use of metal complexes as precursors, etc.) has made it possible to overcome some of the disadvantages listed above. Nevertheless, the search for alternative new methods that ensure uniform distribution of active metal nanoparticles on the support surface is vital for the reduction of the noble metal loading in order to efficiently manage the use of the available noble metal sources.

One of the possibilities to produce such catalytic systems is a newly developed laser electrodispersion (LED) technique. This method has been applied to fabricate thin nanostructured coatings of silicon wafers both naturally and thermally oxidized, with the film being composed of monodispersive and amorphous Cu, Ni, or Pd nanoparticles [3,4]. The most important common feature of the catalysts fabricated by LED is their unusually high activity in the chlorohydrocarbon conversions (Cu and Ni) and hydrogenation (Ni and Pd).

The LED technique belongs to the group of methods that employ bulk metal dispersion rather than atomic aggregation to form metal nanoparticles. Typically, the LED approach allows production not only of vapors but also micrometer and submicrometer drops of the melted metal after the metal target exposure to a pulsed laser beam. These drops enter the laser torch plasma produced near the target surface by optical breakdown of the evaporated target material. The drops become charged in the plasma, and at plasma energies of 20–30 eV their charge achieves a critical value, at which the drops become unstable (Coulomb repulsion force exceeds the surface tension). Unstable drops eject a large number of smaller drops which also overcharge and, thus, produce even smaller drops. Such cascade fission processes result in formation of nanometer-sized droplets, and the fission process terminates at this stage. The nanometer-sized drops cannot keep critical charge (and be unstable) because the flow of electrons emerging from the drop surface starts to exceed that coming in from the plasma. The nanometer-sized droplets undergo solidification at a very high rate and fall on the substrate surface, thus forming amorphous nanoparticles. The process of the metal drops production by LED is described in [5] in more detail.

Detailed investigation of such systems for Pd, Ni, and Cu deposited onto flat (Si, SiO_2/Si, C) and granulated (artificial carbon support Sibunit) supports was performed in a series of works [6–9]. The results can be summarized as follows:

- only size-selected amorphous metal nanoparticles of spherical shape are deposited on the supports;
- the particle size (1–5 nm) is only determined by the metal nature, it does not depend on the support type and the metal loading;
- nanoparticles do not aggregate even within the ensembles of closely packed particles;

- metal nanoparticles are uniformly distributed on the support surface as separated granules or ensembles of closely located granules, and all active sites are available for reagent adsorption;
- nanoparticles are quite resistant to oxidation;
- the surface particle density can be easily controlled by varying the deposition time; and
- a wide range of metals and supports can be used for the catalyst preparation.

All benefits listed above make LED an attractive technique for the production of the catalytic systems. Indeed, as it has been demonstrated currently, the catalysts with a very low metal loading (10^{-3}–10^{-4} % mass) are extremely active in hydrogenation, hydrodechlorination (HDC) (Ni and Pd supported on C or SiO_2), and other catalytic processes; moreover, these systems are very stable in the reaction medium and do not undergo degradation.

Hydrogenation with H_2 is widely used in industry. Usually this reaction proceeds via an adsorptive mechanism that includes adsorption of hydrogen and the reagent. It is commonly believed that hydrogenation reactions are not structure sensitive, i.e., the catalytic properties of the catalyst do not depend on the particle size at the nano-scale. Another type of reduction reaction is the Cl substitution in the molecule with hydrogen (HDC). This reaction also proceeds mainly through adsorption of the reactant and hydrogen on the active metal site, therefore it has many features similar to the hydrogenation reaction, however, it is structure sensitive, as stated by many authors [10–12]. Its structural sensitivity was the main reason to choose HDC as a test reaction for the catalytic properties investigation of the new catalytic systems obtained by LED. Furthermore, this reaction is one of the most attractive existing approaches to disposal of chlorinated wastes owing to its efficiency, aptitude to process all types of chlorinated molecules, fewer energy demands in comparison with oxidation, high speed of transformation, and the intrinsic absence of hazardous byproducts such as dioxins.

The paper in hands deals with the first-time LED preparation of Pd, Ni, and/or Au catalysts on alumina support and the exploration of their material and catalytic properties. These characteristics are compared with the corresponding data for the Pd/C and Ni/C catalytic systems. The catalytic activity was investigated for the gas-phase chlorobenzene (CB) HDC. Transmission electron microscopy (TEM) and X-ray photoelectron spectroscopy (XPS) were used to investigate the structural properties and composition of the catalytic systems before and after the catalytic tests.

EXPERIMENTAL

Pd/C, Ni/C, Pd/Al_2O_3, Au/Al_2O_3, Ni/Al_2O_3, and $Au\text{-}Ni/Al_2O_3$ catalysts were prepared by LED method as described previously [6]. γ-Al_2O_3 (180 m^2/g, AOK-63-11B JSC "Katalizator", grain size about 1 mm) and Sibunit (carbon support [13], 410–406 m^2/g, grain size 2.5–3.0 mm) were used as supports. Pd, Ni, or Au targets were chosen to prepare monometallic Pd, Au, or Ni samples by LED, respectively. Bimetallic $Ni/Au/Al_2O_3$ samples were prepared in a similar way by depositing the Ni nanoparticles onto freshly prepared Au/Al_2O_3; $Au/Ni/Al_2O_3$ was made by deposition of the Au nanoparticles onto Ni/Al_2O_3.

The metal content in the resulting samples was determined by atomic absorption spectrometry (AAS) on a Thermo iCE 3000 AA spectrometer. The metal was preliminarily removed from the support by washing with Aqua Regia ($HCl:HNO_3$ = 4:1). The relative error of the metal content determination was less than 1 %. The data obtained are presented in Table 1.

Table 1 Specific catalytic activity of the catalysts deposited by LED at 200 °C.

Catalyst	M loading, % mass[a]	Mean metal particle size (TEM), nm	CB conversion, %	Activity, mol CB(mol M × h)
Carbon support (Sibunit)				
Pd/C-1	1.1×10^{-4}	2	87	800 000
Pd/C-2	7×10^{-4}	2	87	200 000
Pd/C-3	1.1×10^{-3}	2	78	66 000
Pd/C-4	3×10^{-3}	2	37	21 000
Pd/UDD-Imp.[b]	0.5	2–3	100	570
Ni/C-1	1.3×10^{-3}	2	33	27 800
Ni/C-2	2.6×10^{-3}	2	10	9500
Alumina support				
Pd/Al_2O_3	1×10^{-2}	2	100	22 000
Ni/Al_2O_3-1	1.1×10^{-3}	2	70	41 600
Ni/Al_2O_3-Imp.[c]	4	2	75	23
Au/Al_2O_3-1	0.009	2	30	7000
$Ni/Au/Al_2O_3$-1	0.009Au			
	0.0011Ni	2–8	22	3710
$Au/Ni/Al_2O_3$	0.009Au			
	0.0011Ni	2–8	72	12 000

[a]Found by AAS.
[b]Prepared by wet impregnation of UDD with a $Ni(NO_3)_2$ solution.
[c]Prepared by wet impregnation of alumina with a $Ni(NO_3)_2$ solution.

The Brunauer–Emmett–Teller (BET) surface area, the pore size distribution, and the total pore volume were determined by N_2 adsorption/desorption isotherms at 77 K on Quantachrome Autosorb 1. The pore size distributions were calculated using the desorption branch of the N_2 isotherm and the Barret–Joyner–Halenda (BJH) method [14]. Neither the BET surface area characteristic for the alumina (180 m^2/g) and the carbon support (410–406 m^2/g) nor the pore structure changed noticeably after the metal deposition.

High-resolution transmission electron microscopy (HRTEM) investigation was carried out with a JEOL JEM 2100F microscope operated at 200 kV. High angle annular dark field mode (HAADF) and energy-dispersive X-ray spectroscopy (EDX) were applied to study the catalyst morphology and composition. Three hundred particles of the supported metal were processed to determine the particle size distribution and the mean particle diameters for each catalyst. Two types of samples were prepared for the HRTEM spectroscopy. Ni alone or Au and Ni together were deposited directly on the Cu grids holding the TEM samples to produce the first type of samples. The outer layers of the catalyst granules on alumina, which contained most of the metal particles, were scraped off by scalpel and deposited on a Cu-holder from an ultrasonic treated water suspension to produce the second type of samples.

X-ray photoelectron spectra of the catalysts were obtained using Kratos XSAM-800 and Axis Ultra DLD spectrometers with monochromatic Al Kα radiation for the spectra excitation. The binding energy scale was calibrated using the following peak positions: Au $4f_{5/2}$ – 83.96 eV, Cu $2p_{3/2}$ – 932.62 eV, Ag $3d_{5/2}$ – 368.21 eV, Pt $4f_{7/2}$ – 90.99 eV.

The HDC of CB (Acros Organics, 99.5 %) was performed in a flow-type fixed-bed reactor. The mixture of CB and hydrogen was prepared by passing H_2 through a bubbler with CB; the reagents were supplied into the reactor from below. The rate of CB supply (recalculated per metal weight in the catalyst) was 1.1 h^{-1} in all experiments. The catalyst weight was 50 mg, and the H_2 flow rate was 35 ml/min. No preliminary reduction of the samples was performed. The catalytic tests were performed

at a stepwise temperature increase (and in some experiments also decrease): after a constant conversion at a given temperature was achieved, the introduction of CB + H_2 mixture was switched over to supply only the H_2 flow, and the temperature of the reactor was increased to the next value. This procedure was used to measure the catalytic activity over the temperature range 30–350 °C. The analysis samples were periodically taken from the upper part of the reactor using a syringe. They were analyzed by gas chromatography (GC) with a DBWax capillary column (30 m) and a flame ionization detector on an Agilent 6890N GC device.

RESULTS AND DISCUSSION

HRTEM characterization

As it was demonstrated previously for Pd, Ni, and Cu deposited on C, Si, and SiO_2/Si [3,6], the size of the metal nanoparticles deposited on the support by the LED method depends on the metal nature only: the mean particle size of Pd is about 2.1 nm, Ni forms particles about 2.3 nm in size, for Cu this value is equal to 5 nm. However, so far no Au nanostructures obtained by LED have been reported. Besides, Al_2O_3 has never been used before to prepare catalysts by LED. Therefore, the information on the structure of Ni/Al_2O_3, Au/Al_2O_3, and bimetallic Au/Ni containing samples, especially on the mean size and the size distribution, is of prime importance.

LED catalysts are of core-shell type [7] with very low metal content, as illustrated in Table 1. For this reason, after crashing the catalyst granules it would be hardly possible to observe the metal nanoparticles by HRTEM. Therefore, special model systems that contain Ni or Ni and Au particles deposited by LED onto Cu-holder for TEM samples were investigated. The corresponding TEM images of the Ni/Cu-holder are shown in Fig. 1 (in Fig. 1A, an HAADF scanning TEM image is presented). It is clearly seen from Figs. 1A,B, as well as from the diagram of the particle size distribution presented as an insert in Fig. 1B, that the size of the Ni particles is 1.5 ± 0.5 nm. Narrow particle size distribution is in accordance with the data previously obtained for Ni on Si supports in [6], however, in our case the mean particle size is smaller than in the cited paper (1.5 vs. 2.3 nm). Also, short chains formed by Ni particles are clearly seen in Fig. 1A, which is also in accordance with the previous findings for the Ni/SiO_2 system obtained by LED [6].

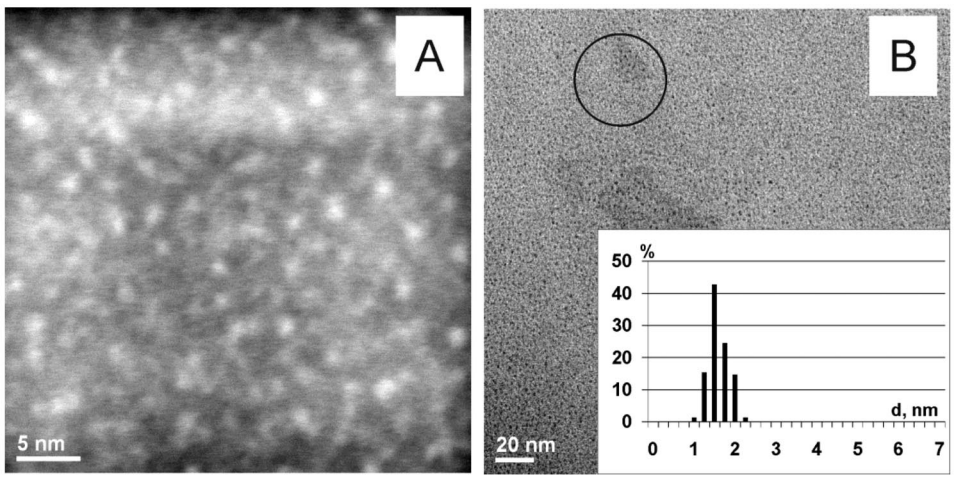

Fig. 1 HRTEM microphotographs of Ni/Cu-holder with different magnification (A, B), and a diagram of particle size distribution (B).

Figures 2A–C shows with increasing magnification the HRTEM images of the bimetallic system of Ni/Au on a Cu-holder, Fig. 2D demonstrates the particle size distribution for this sample. The EDX study was performed to distinguish the Au and Ni particles (spot size was 1 nm in diameter). Analysis of the whole image area (900 nm^2) demonstrates the presence of both Ni and Au, and the data obtained for selected points demonstrate also the presence of both Ni and Au in variable quantities, i.e., a certain compositional non-uniformity was observed (in total, 17 points were analyzed). According to preparation technique and the AAC data presented in Table 1, the total (or mean) Au:Ni ratio in the sample was about 10:1; the Au:Ni ratio detected by EDX for different points was in the range of 10:1 to 5:1 (Fig. 2E). Almost no points that contain only Au or only Ni were detected. This result can be explained both by bimetallic particles formation and deposition of individual Au and Ni particles so close to each other that it becomes impossible to distinguish them.

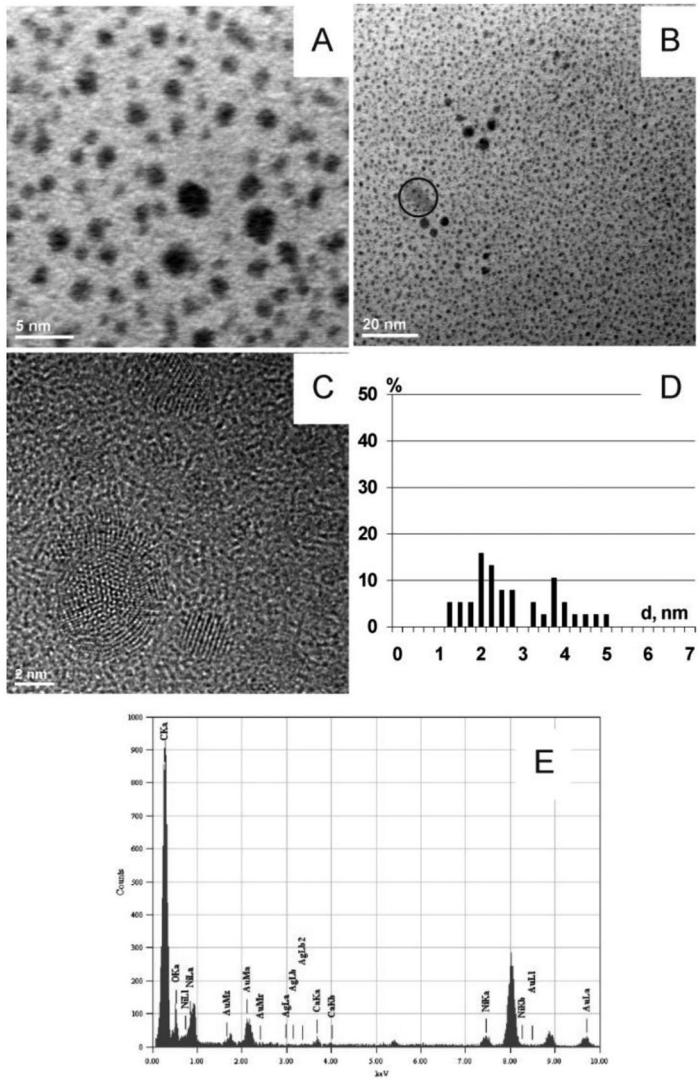

Fig. 2 HRTEM microphotographs with different magnification (A, B, C) and particle size distribution (D) for Ni/Au deposited on Cu-holder.

Although most of the particles in the Ni/Au/Cu-holder sample are nearly of the same size (the mean particle size is very close to that in the Ni/Al_2O_3 sample), there is a fraction with larger sizes, as clearly seen in Fig. 2B. Thus, broader particle size distribution in the range 1–5 nm is characteristic of this sample. Such wide particle size distribution obtained for the Ni/Au/Cu-holder sample is unusual for systems prepared by the LED method.

HRTEM investigation of model samples prepared by direct LED of active metal on the Cu-holder for TEM demonstrates the presence of nanosized metal particles with practically uniform distribution. During preparation, the metal particles are formed before they reach the support surface, therefore, we expect the same size distribution for alumina-supported samples. To check this, the second type of TEM samples was prepared by scribing the catalyst granule surface (as described in the Experimental section). The corresponding HRTEM images for Au/Al_2O_3 are presented in Fig. 3. Round-shaped Au particles of 1–8 nm in size were found in Au/Al_2O_3; they are very similar to those found in the Ni/Au/Cu-holder sample. A fraction of round particles joint into short chains (2–5 particles) was also observed. Especially clear images were produced by HAADF. Besides, around the particles certain wide bright regions were observed in the TEM images. This may be explained by the presence of very fine particles on the alumina surface, down to atomic Au. Similar regions are present on the Cu-holder-supported samples (round marks in Figs. 1B and 2B). It seems that such fine particles may be possibly formed by the LED method, however, it has not been demonstrated before. Significant broadening of the Au 4*f* peaks in the XPS spectra of the same sample (see the XPS discussion section) confirms the formation of such subnanoparticles.

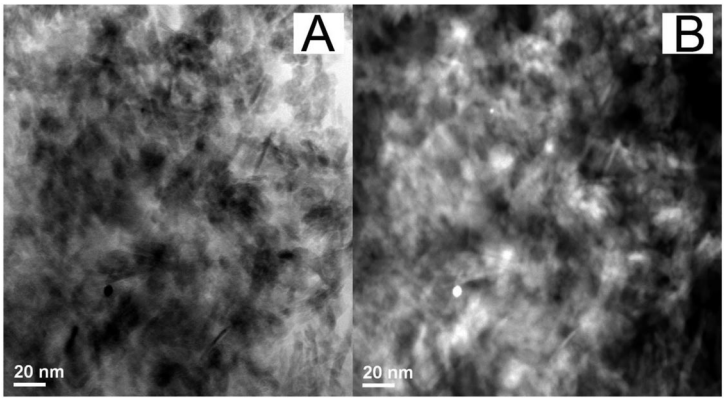

Fig. 3 HRTEM microphotographs for Au/Al_2O_3: transmission (A) and STEM-HAADF (B) image.

Ni/Al_2O_3 was also investigated by HRTEM, however, no metal particles were found in this sample (images are not presented here). The EDX analysis demonstrates the presence of Ni; therefore, Ni is most likely present in an oxidized state. It is difficult to distinguish the oxidized Ni particles in the TEM images from the alumina particles that dominate in the sample. Oxidation of Ni particles could proceed due to interaction with the alumina support during preparation. When metal particles are sputtered during LED, their speed is very high, and Ni oxidation may take place owing to local overheating when it collides with the alumina surface that contains an ample amount of oxygen. Possible oxidized forms of Ni could be NiO or $NiAl_2O_4$; formation of aluminate in alumina-supported Ni catalysts was found in many works [15,16]. The presence of oxidized Ni in Ni/Al_2O_3 was confirmed by XPS. Thus, alumina-supported Ni differs from Ni/C prepared by LED, as well as from the Ni/Cu-holder samples. Both metallic Cu-holder for TEM and Sibunit carbon material used as a carbon support do not contain oxygen, so only Ni(0) particles were observed in these samples. It was demonstrated in [4] that Ni in

Ni/C is in a metal state, and Ni nanoparticles are very resistant to oxidation during storage in air (more than 6 months). This is also valid for the Pd/C catalysts prepared by LED. Pd nanoparticles in these samples (with different Pd loading, see samples Pd/C-1 to Pd/C-4 in Table 1) are also very resistant to air oxidation. The TEM images of such catalysts are presented elsewhere [7]; very narrow particle size distribution with a mean size of about 2.1 nm was found for Pd/C with Pd loading in the range 1.1×10^{-4} to 3×10^{-3} % mass. Thus, the alumina-supported catalysts have a characteristic feature that distinguishes them from the carbon-supported LED systems, i.e, a higher oxidation degree of Ni owing to the Ni-support interaction. Wider Au particle size distribution in comparison with other LED dispersed metals was found not only on alumina, but also on other supports (e.g., carbon). It was also found for the first time that the maximum of the particle size distribution for Ni particles produced by LED is not a constant value, as it seemed to be the case. For example, in the Ni/Cu-holder sample the mean particle size is smaller (1.5 nm) than in the previously studied Ni/SiO_2 system (2.3 nm).

Catalyst studies by XPS

XPS data for the LED catalysts are summarized in Table 2. According to the XPS results, which are presented in more detail in the previous work [7], the Pd $3d_{5/2}$ peak position (336.1 eV) and the corresponding line shape confirm that only Pd(0) is presented in Pd/C prepared by LED after its brief activation in H_2 (150 °C, 30 min). When comparing the XPS spectra of Pd/C and Pd/Al_2O_3 (Fig. 4), one may see the presence of a significant amount of PdO together with metallic Pd for the samples under discussion. We may conclude that the interaction of Pd nanoparticles produced by LED with the oxide support leads to partial oxidation of the noble metal (Pd), which is not observed for the carbon support.

No indications of Au oxidation on the alumina support were found by XPS. As shown in Table 2, the binding energy for the Au $4f_{7/2}$ peak is nearly the same for Au/Al_2O_3, the bimetallic catalysts and the Au foil. As it was demonstrated by TEM, Au is present in the catalysts both as nanoparticles 1–8 nm in size and as fine particles of a nearly atomic size. It is known that the metal binding energy may be shifted by about 1 eV owing to well-known size effects [18]. The absence of the energy shift could be associated with the presence of atomic conductive gold layer that forms the "foil" layer on the alumina surface.

Table 2 Results of XPS study of alumina-supported Pd, Ni, and/or Au catalysts deposited by LED.

Catalyst	E_B, eV before/after the catalytic test		
	Pd 3*d*	Ni 2*p*	Au 4*f*
Pd/C-4	336.1–336.1		
Ni/Al_2O_3-1		856.08–856.4	
Au/Al_2O_3-1			83.9–84.12
$Au/Ni/Al_2O_3$		856.23–856.39	84.19–84.39
Pd foil	336.0		
PdO			
$PdCl_2$			
Au foil			83.7–84.0
Au_2O_3			85.9
Ni foil	852.7		
NiO		856.0[a]	
$NiAl_2O_4$	856.2		

[a]Ni foil oxidized by O_2 [17].

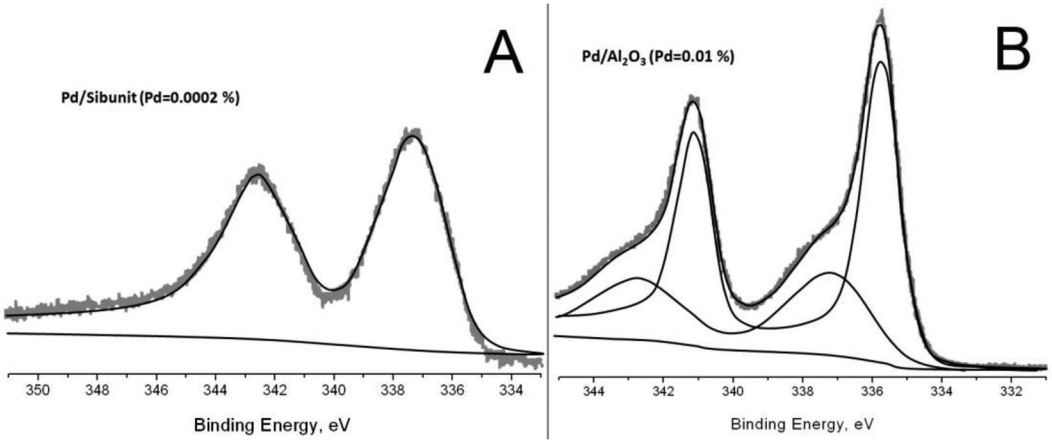

Fig. 4 Pd $3d_{5/2}$ XPS spectra for Pd/C (A) and Pd/alumina (B) prepared by LED.

The Ni $2p_{3/2}$ binding energy in Ni/Al_2O_3 and $Au/Ni/Al_2O_3$ is 856 eV, which corresponds to NiO or $NiAl_2O_4$, while for metallic Ni the binding energy is lower (852.7 eV). Thus, the XPS data confirm the suggestion about possible interaction between alumina and Ni particles deposited by LED, which leads to Ni oxidation.

Gas-phase hydrodechlorination of chlorobenzene on LED-prepared catalysts

Catalytic properties of the LED catalysts were studied for the reaction of the gas-phase HDC of CB. The reaction proceeds according to the scheme given below:

$$C_6H_5Cl + H_2 \rightarrow C_6H_6 + HCl$$

Further hydrogenation of benzene could lead to cyclohexane formation, but this side reaction does not take place on the LED-prepared catalysts investigated in this work. Benzene was the only product in the presence of all catalysts.

Specific catalytic activity and conversion rate of CB on the catalysts at 200 °C are given in Table 1. Data for the 4 % Ni/Al_2O_3 (Ni/Al_2O_3-Imp.) and 0.5 % Pd/UDD (Pd/UDD-Imp.) (UDD is ultradispersed diamond) prepared by wet impregnation from nitrate are presented for comparison. As it has been demonstrated previously, the UDD-supported catalyst with a 0.5 % Pd loading contains 1–3 nm Pd particles, and it was the most active both in the liquid-phase HDC of 1,3,5-trichlorobenzene and the gas-phase HDC of CB in comparison with the catalysts with higher Pd loading (1–5 % mass) or those supported by other carbon carriers [19].

Specific catalytic activity of the LED catalysts was found to be extremely high compared to Pd/UDD-Imp. and Ni/Al_2O_3-Imp. prepared by the impregnation method. The specific catalytic activity of LED catalysts forms the following sequence:

$Pd/C \approx Pd/Al_2O_3 > Ni/Al_2O_3 > Ni/C > Au/Ni/Al_2O_3 > Au/Al_2O_3 > Ni/Au/Al_2O_3 >$ 0.5 % Pd/UDD-Imp. > 4 % Ni/Al_2O_3-Imp.

This result most likely can be explained as follows: (1) the core-shell structure of the granulated catalysts where all metal particles (very small and uniformly distributed) are situated on the outer surface and therefore are easily accessible for the reagents adsorption; (2) there is possible charge transfer between adjacent metal particles or a metal particle and the conductive support (as in the case of the carbon support) owing to tunnel electron transfer (this reason is discussed in [4] in detail). HDC is

known to be a structure-sensitive reaction. So, the mean metal particle size is an important factor to achieve high activity. It should be underlined that the Ni oxidized state in Ni/Al_2O_3 and the bimetallic catalysts (based on the TEM and XPS data) does not hamper the catalytic reaction. No specific reduction before the catalytic tests was performed. It seems that Ni can be reduced by H_2 in the reaction medium. Indeed, the conversion of CB on Ni/Al_2O_3 increases as the reaction temperature increases from 100 to 350 °C. However, such improvement is even more pronounced for Ni/C, in which Ni is present in the metal state. Activity of this catalyst is lower than that of the alumina-supported Ni (Fig. 5) in the whole temperature range under investigation (100–300 °C). It could be proposed that the oxidized form of Ni (such as the surface NiO or rather aluminate) is active in the HDC reaction. As shown by XPS, the oxidized form of Pd is also present in Pd/Al_2O_3, but in this case it is hard to find a difference between the alumina- and carbon-supported Pd owing to high intrinsic activity. It should be noted that there are certain data on the possible improvement of the metal catalyst activity in HDC reactions owing to improvement of the chlorinated reagent adsorption when Pd is partially oxidized [20].

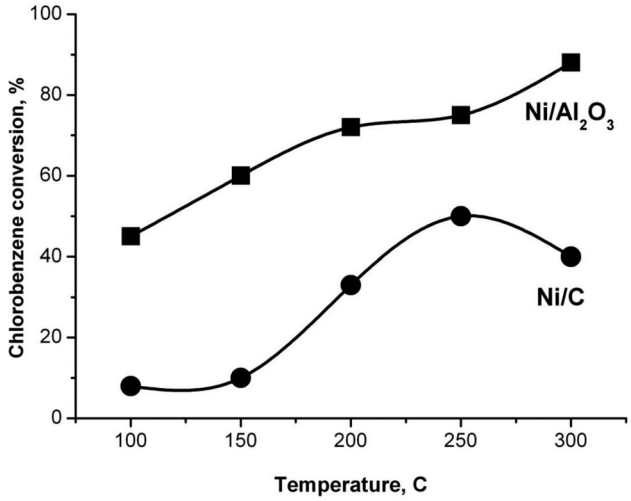

Fig. 5 Comparison of the CB conversion vs. the reaction temperature for alumina- and C-supported Ni catalysts prepared by LED.

As it also follows from Table 1, generally the decrease of the metal content causes the improvement in the specific catalytic activity. The CB steady-state conversion at a given temperature first increases, then reaches a certain value and becomes stable as the metal loading decreases, which is clear from comparison of the Pd/C-1 to Pd/C-4 samples.

As for the Au-containing systems, the TEM data demonstrate a broader particle size distribution. Au was found to be catalytically active only at a certain metal particle size (1.5–3 nm) [21]. Since in Au/Al_2O_3 the particle size varies from 1 to 8 nm, probably not all Au particles are involved in the catalytic reaction. Besides, the activity of Au in the reductive reaction is lower than for Ni and especially Pd, which is able to absorb ample amounts of H_2. Another reason for the low catalytic activity is the presence of a layer of very fine Au particles (down to an atomic size) that was found by TEM and confirmed by XPS in Au-containing catalysts supported on Al_2O_3. It was already mentioned that the tunnel electron transfer between the metal particles and the formation of highly active charged particles could lead to high catalytic activity of the LED systems. The presence of atomic Au creates a conductive surface and makes the electron-transfer effects less significant. As a result, the catalytic activity for Au LED catalysts is lower than for the Ni-containing ones.

Specific activity of the Au/Ni bimetallic catalysts was significantly lower than that of Ni/Al_2O_3. Besides, the catalytic activity depends on the deposition sequence. During preparation of $Ni/Au/Al_2O_3$, Au was deposited first, and Ni afterwards; specific activity of the catalyst prepared in such a way was three times less in comparison with the catalyst $Au/Ni/Al_2O_3$, which was prepared using the opposite deposition sequence. Specific activity of Au/Al_2O_3 is intermediate in comparison with the two bimetallic samples. It seems that Au deposition on Ni/Al_2O_3 leads to partial covering of the active Ni particles with Au, and this process causes the decrease of the specific catalytic activity in comparison with Ni/Al_2O_3. On the other hand, it was found by TEM and confirmed by XPS that Ni is present on the alumina surface mostly in the oxidized state, probably as oxide or spinel. If Au particles are deposited on such a modified surface, their properties can change significantly and thus cause the changes in the catalytic activity.

When Au is deposited first, the formation of a layer of atomic Au totally changes the Ni deposition mechanism. It was found in [21] that Ni particles deposited by LED on a Au surface display tendency to self-organization, thus forming spirals and nets. Formation of such ensembles may also negatively affect the catalytic activity. Besides, the presence of conductive Au film could suppress the inter-particle charge transfer and thus lower the catalytic efficiency significantly.

The layer of super-finely distributed Au particles could disappear due to aggregation at the temperature increase during the catalytic test. This may contribute to the improvement of the $Au/Ni/Al_2O_3$ and $Ni/Au/Al_2O_3$ catalytic activity with the temperature increase (CB conversion is 10 and 43 % at 150 °C vs. 22 and 73 % at 200 °C for $Ni/Au/Al_2O_3$ and $Au/Ni/Al_2O_3$, correspondingly).

It should be emphasized that Pd-, Ni-, and even Au-containing catalysts prepared by LED are much more active in the CB HDC than Ni and even Pd catalysts prepared by wet impregnation with a much higher metal content. This fact confirms great capabilities of the LED method for preparation of highly active catalysts with simultaneous cost saving owing to significant decrease of the metal loading. Another important issue for the industrial catalysts is stability in the reaction conditions. In Fig. 6, the CB conversion vs. time-on-stream is presented for Pd/Al_2O_3, $Ni/Au/Al_2O_3$, and $Au/Ni/Al_2O_3$ LED catalysts.

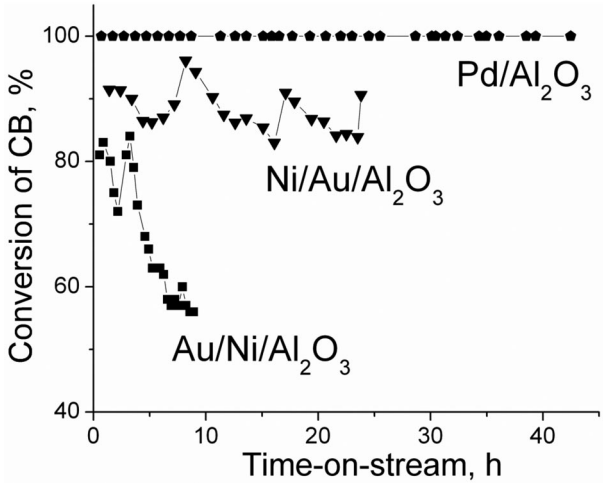

Fig. 6 Conversion of CB vs. time-on-stream Pd/Al_2O_3 (250 °C), $Au/Ni/Al_2O_3$, (200 °C), and $Ni/Au/Al_2O_3$ (300 °C).

As it can be seen from Fig. 6, Pd/Al_2O_3 catalyst is very stable, and a 100 % CB conversion was observed during 45 h time-on-stream at 250 °C. $Ni/Au/Al_2O_3$ was less stable, although stability testing was performed at 300 °C. During each testing day, the conversion decreased slightly from ≥90 to 82–85 %, however, every time it recovered to the initial value of 90 % after the night break.

During catalytic test for $Au/Ni/Al_2O_3$ at 200 °C, the decrease of conversion vs. time-on-stream was more significant, from 83 to about 53 % during 5 h, but after the night break the conversion restored to its maximum. A nearly equal conversion of about 53 % was maintained during at least 3 h. This catalyst may be reactivated by reduction with H_2 at 300–350 °C. One can conclude that at higher temperature, which is close to the NiO reduction temperature (300 °C), the Ni-containing samples are more stable than at 200 °C. Recently, prolonged testing at 300 °C of another $Au/Ni/Al_2O_3$ sample containing reduced metals loading (one-half of Au and Ni loading in comparison with the sample described above) was performed (not shown in this article). The activity was lower in this case but also decreased during catalytic test (from ≥70 to 30–35 %) and every time it recovered to the value of 50 % after the night break. A 30–35 % stable-state CB conversion was observed during 15 h time-on-stream at 300 °C.

This fact, as well as the increase of CB conversion at the beginning of the reaction, points to activation of the active sites by the reaction mixture. It is clearly seen from Fig. 6 that LED catalysts are quite stable in CB HDC, although HCl evolving during the reaction could oxidize the metal nanoparticles, and especially the Ni nanoparticles, which are not as resistant to oxidation as noble metals. To clarify this subject, the XPS analysis of the samples before and after the catalytic tests was performed.

Catalytic performance in HDC is usually accompanied with chlorination of the active metal [22,23] and the support [24] that results in the catalyst deactivation. The Au $4f_{7/2}$ binding energy in AuCl is about 84.6 eV, therefore, a slight shift of the Au 4*f* line in Au-containing catalysts to higher values after the catalytic tests (83.9/84.12 and 84.19/84.39 before/after the catalytic test for Au/Al_2O_3-1 and $Au/Ni/Al_2O_3$, correspondingly) could be attributed to a slight chlorination of Au. To clarify this question, the Cl content on the catalyst surface was estimated from the XPS data. The catalyst surface composition before and after the catalytic tests in the CB HDC is shown in Table 3.

Table 3 Surface composition for $Ni/Au/Al_2O_3$ according to the XPS data.

Catalyst	Content, % mass						Relative ratio	
	Al 2*p*	O 1*s*	C 1*s*	Au 4*f*	Ni 2*p*	Cl 2*p*	Au/Ni	Au/Al
Au/Al_2O_3	10.1	23.7	64.9	1.3	–	–	–	0.13
Au/Al_2O_3 after HDC	16.0	69.6	8.4	5.8	–	0.2	–	0.36
$Au/Ni/Al_2O_3$	18.3	27.6	50.0	2.6	1.5	–	1.7	0.082
$Au/Ni/Al_2O_3$ after HDC	23.4	57.4	13.2	4.5	1.3	0.2	3.5	0.19
Ni/Al_2O_3	18.3	52.9	18.9	–	9.9	–	–	–

Since the catalysts were prepared by LED, no Cl is present in the pristine catalysts. Some residual Cl is usually found in catalysts prepared by traditional method from chlorides as metal precursors [25,26]. The amount of Cl on the catalyst surface is also very low after the catalytic tests. For the tested Pd-containing catalyst, the Pd oxidation state does not change during the catalytic test in the CB HDC. Neither PdO nor $PdCl_2$ were found in the sample after 7 h time-on-stream. Moreover, the amount of Cl on the surface of Pd/C remains insignificant after the catalytic test (Cl/C = 0.01). For Ni/Al_2O_3 after the catalytic test during 8 h Cl/alumina = 0.05.

Similar results were found for less active alumina-supported bimetallic Au/Ni catalysts. It could be supposed that the catalyst stability is connected with high concentration of the active metal on the outer surface of the catalyst granules. In this case, a fast Cl desorption (via HCl formation) proceeds on

the surface. This effect is especially pronounced for Pd catalysts owing to high H_2 absorption capacity of Pd. After the catalytic test, the Au $4f_{7/2}$ binding energy increases slightly, whereas there is no Ni $2p_{3/2}$ peak position shift. Such changes may be caused by aggregation of the atomic Au in clusters or by metal chlorination during the reaction. After sintering, the conductive layer disappears and the Au $4f_{7/2}$ binding energy slightly shifts toward higher values. The disappearance of Au atomic layer should change the catalytic properties of the bimetallic catalysts, so that their properties become similar to those of Ni/Al_2O_3.

One can conclude that the LED catalysts are resistant toward oxidation during the HDC reaction. This result is in good agreement with the data reported in [7], where the stability of the LED particles toward oxidation was explained by an amorphous state of the metal and a small size of the metal nanoparticles.

CONCLUSIONS

LED of metals on commonly used carbon or oxide supports can be used to produce core-shell catalysts nanoparticles of a uniform size distributed on the granule surfaces. Such catalysts have a very high specific catalytic activity. Besides, they are very stable in the HDC reaction. Such systems are a promising alternative to those produced by the "wet chemistry" methods, owing to a number of advantages such as no need to use metal chlorides or nitrates, very low loadings of noble or base metals (up to 10^{-4} % mass), improvement of the catalytic performance at decreased metal loading, resistance toward the reaction medium, and a wide range of possible applications.

ACKNOWLEDGMENTS

The authors appreciate the financial support through Grants of Russian Ministry of Science and Education #02.740.11.0026 and RFBR (#10-03-00372 and #11-03-00403).

REFERENCES

1. G. Ertl, H. Knözinger, F. Schüth, J. Weitkamp (Eds.). *Handbook of Heterogeneous Catalysis*, Vol. 1, 2nd ed., p. 4270, John Wiley (2008).
2. Y. J. Huang, J. A. Schwarz. *Appl. Catal.* **30**, 255 (1987).
3. V. M. Kozhevin, D. A. Yavsin, V. M. Kouznetsov, V. M. Busov, V. M. Mikushkin, S. Yu. Nikonov, S. A. Gurevich, A. Kolobov. *J. Vac. Sci. Technol., B* **18**, 1402 (2000).
4. S. A. Gurevich, V. M. Kozhevin, I. N. Yassievich, D. A. Yavsin, T. N. Rostovshchikova, V. V. Smirnov. *Thin Films and Nanostructures: Physico-Chemical Phenomena in Thin Films and at Solid Surfaces*, L. I. Trakhtenberg, S. H. Lin, O. J. Ilegbusi (Eds.), Elsevier, Amsterdam, **34**, 726 (2007).
5. T. N. Rostovshchikova, S. A. Nikolaev, E. S. Lokteva, S. A. Gurevich, V. M. Kozhevin, D. A. Yavsin, A. V. Ankudinov. *Stud. Surf. Sci. Catal.* **175**, 263 (2010).
6. T. N. Rostovshchikova, V. V. Smirnov, S. A. Gurevich, V. M. Kozhevin, D. A. Yavsin, S. M. Nevskaya, S. A. Nikolaev, E. S. Lokteva. *Catal. Today* **105**, 344 (2005).
7. E. S. Lokteva, T. N. Rostovshchikova, S. A. Kachevskii, E. V. Golubina, V. V. Smirnov, A. Yu. Stakheev, N. S. Telegina, S. A. Gurevich, V. M. Kozhevin, D. A. Yavsin. *Kinet. Catal*. **49**, 748 (2008).
8. V. Lunin, V. Smirnov, E. Lokteva, T. Rostovshikova, S. Kachevsky. In: *The Role of Ecological Chemistry in Pollution Research and Sustainable Development. Proceedings of the NATO Advanced Research Workshop, Chisinau, Moldova*, A. M. Bahadir, G. Duca (Eds.), pp. 221–232, Springer, Amsterdam (2008).

9. T. N. Rostovshchikova, V. V. Smirnov, V. M. Kozhevin, D. A. Yavsin, M. A. Zabelin, I. N. Yassievich, S. A. Gurevich. *Appl. Catal., A* **296**, 70 (2005).
10. T. Mori, T. Yasuoka, Y. Morikawa. *Catal. Today* **88**, 111 (2004).
11. E. Diaz, L. Faba, S. Ordonez. *Appl. Catal., B* **104**, 415 (2011).
12. J. W. Bae, I. G. Kim, J. S. Lee, K. H. Lee, E. J. Jang. *Appl. Catal., A* **240**, 129 (2003).
13. Y. I. Yermakov, V. F. Surovikin, G. V. Plaksin, V. A. Semikolenov, V. A. Lokholobov, A. L. Chuvilin, S. V. Bogdanov. *React. Kinet. Catal. Lett.* **33**, 435 (1987).
14. E. P. Barret, L. G. Joyner, P. P. Halenda. *J. Am. Chem. Soc.* **73**, 373 (1951).
15. E. Heracleous, A. F. Lee, K. Wilson, A. A. Lemonidou. *J. Catal.* **231**, 159 (2005).
16. M. Garcia-Dieguez, E. Finocchio, M. F. Larrabia, L. J. Slemany, G. Busca. *J. Catal.* **274**, 11 (2010).
17. NIST X-Ray Photoelectron Spectroscopy Database, Version 3.5, National Institute of Standards and Technology. Gaithersberg, MD (2003). <http://srdata.nist.gov/xps/>
18. I. Lopez-Salido, D. Ch. Lim, Y. D. Kim. *Surf. Sci.* **588**, 6 (2005).
19. E. V. Golubina, S. A. Kachevsky, E. S. Lokteva, V. V. Lunin, P. Canton, P. Tundo. *Mendeleev Commun.* **19**, 133 (2009).
20. L. M. Gomez-Sainero, X. L. Seoane, J. L. G. Fierro, A. Arcoya. *J. Catal.* **209**, 279 (2002).
21. R. Zanella, C. Louis, S. Giorgio, R. Touroude. *J. Catal.* **223**, 328 (2004).
22. M. A. Alvarez-Montero, L. M. Gomez-Sainero, J. Juan-Juan, A. Linares-Solano, J. J. Rodriguez. *Chem. Eng. J.* **162**, 599 (2010).
23. N. Lingaiah, Md. A. Uddin, A. Muto, Y. Sakata. *Chem. Commun.* 1657 (1999).
24. M. A. Aramendia, V. Borau, I. M. Garcia, C. Jimenez, A. Marinas, J. M. Marinas, F. J. Urbano. *J. Catal.* **187**, 392 (1999).
25. H. Karhu, A. Kalantar, I. J. Väyrynen, T. Salmi, D. Yu. Murzin. *Appl. Catal., A* **247**, 283 (2003).
26. E. S. Lokteva, A. E. Lazhko, E. V. Golubina, V. V. Timofeev, A. V. Naumkin, T. V. Yagodovskaya, S. N. Gaidamaka, V. V. Lunin. *J. Supercrit. Fluids* **58**, 263 (2011).

